ELSEVIER
IFAC
PUBLICATIONS
www.elsevier.com/locate/ifac

VAN DE VUSSE CSTR AS A BENCHMARK PROBLEM FOR NONLINEAR FEEDFORWARD CONTROL DESIGN TECHNIQUES

Knut Graichen Veit Hagenmeyer [1] Michael Zeitz

Institut für Systemdynamik und Regelungstechnik,
Universität Stuttgart, Germany
{graichen,hagenmeyer,zeitz}@isr.uni-stuttgart.de

Abstract: The finite–time transition between equilibrium points of the isothermal Van de Vusse CSTR model is considered as a benchmark scenario to present two design approaches of nonlinear feedforward control which do not distinguish between minimum–phase and nonminimum–phase systems in contrast to conventional system inversion techniques. Firstly, since the CSTR model is differentially flat, the flatness–based design can be applied. Secondly, a new approach presented in this contribution treats the transition task as a two–point boundary value problem of the internal dynamics which can be numerically solved by a standard MATLAB function. The two design approaches of nonlinear feedforward control are illustrated for the open–loop tracking control of the CSTR model.

Keywords: system inversion, internal dynamics, nonminimum–phase, feedforward control, setpoint–transition, flat system, boundary value problem

1. INTRODUCTION

In many industrial applications, model–based feedforward control is used to improve the desired tracking performance e.g. of position or load changes for mechatronical systems or in process control. In comparison to the broad spectrum of available design methods for feedback control, only few methods are known for designing feedforward control in contrast to the respective demand in industry. The reason for this methodological gap is related to the system inversion required in course of the feedforward control design and the respective difficulties arising with nonlinear systems.

The system inversion in context with feedforward control design has been thoroughly investigated by Devasia, Chen, and Paden (Devasia *et al.*, 1996; Chen and Paden, 1996) who also initiated a series of further contributions (Hunt and Meyer, 1997; Devasia and Paden, 1998; Devasia, 1999; Zou and Devasia, 1999; Taylor and Li, 2002). The developed stable inversion technique distinguishes whether the considered system is minimum–phase or nonminimum–phase, because the internal dynamics must be numerically solved in order to determine the nominal input trajectory. If the internal dynamics is unstable, a reverse–time integration is applied such that the solution and the respective input trajectory do not become unbounded. In this case, the input trajectory is noncausal, i.e. the feedforward control has to start in advance to realize a finite–time transition, and is therefore only approximately realizable.

In (Perez *et al.*, 2002), an isothermal continuous stirred tank reactor (CSTR) model with the Van de Vusse reaction has been used as a challenging benchmark problem with nonminimum–phase

[1] V. Hagenmeyer (BASF AG, Ludwigshafen) was at Universität Stuttgart, when the article was written.

behavior, where the constraints of the stable system inversion technique utilized for feedforward design become evident. Thereby, the transitions between equilibrium points which are needed in process control during startups, shutdowns, and load changes have been studied in order to illustrate feasible and non–feasible transitions.

In this contribution, the nonlinear Van de Vusse CSTR model is used to present two alternative design techniques for feedforward control, which enable a finite–time transition between all equilibrium points and deliver causal and implementable input trajectories. Since the considered CSTR model is differentially flat (Fliess *et al.*, 1995), the flatness–based design of the feedforward control is applied as a first alternative. The determination of the nominal input trajectory is purely algebraic and requires no time integration, if the transition task is formulated in the coordinates of the flat output (Fliess and Marquez, 2000; Hagenmeyer and Zeitz, 2004).

The second design approach developed by the authors (Graichen *et al.*, 2004) treats the transition between equilibrium points as a two–point boundary value problem (BVP) throughout all design steps of the inversion–based feedforward control. The main idea concerns that the predefined output trajectory provides free parameters which are necessary for the solvability of the BVP of the internal dynamics. This BVP with unknown parameters can be solved numerically by a standard MATLAB function.

The paper is outlined as follows. At first, the considered feedforward control task is explained for the isothermal CSTR with the Van de Vusse reaction. Then, the application of the stable inversion technique for feedforward control design used in (Perez *et al.*, 2002) is shortly recapitulated in order to motivate the presentation of the two other approaches. The different design techniques are illustrated by discussion and simulation results for the feedforward tracking control of the CSTR model.

2. TRANSITION CONTROL PROBLEM OF THE VAN DE VUSSE CSTR

The Van de Vusse scheme $A \rightarrow B \rightarrow C$, $2A \rightarrow D$ comprises two reactions of the monomer A to the product B and to the undesired byproducts C and D. The material balances of A and B

$$\dot{c}_A = -k_1 c_A - k_3 c_A^2 + (1 - c_A)u, \qquad (1)$$

$$\dot{c}_B = k_1 c_A - k_2 c_B - c_B u \qquad (2)$$

are formulated for the concentrations $c_A(t)$ and $c_B(t)$ which are normalized by the input concentration c_{A0}.[2] The reaction parameters $k_i, i = 1, 2, 3$ are positive constants due to the isothermal operation of the CSTR. The input $u(t)$ of the CSTR is the dilution rate of the reactant A with the inlet concentration c_{A0} and is constraint to be between $10\mathrm{h}^{-1} \leq \mathrm{u} \leq 400\mathrm{h}^{-1}$. The output $y(t) = c_B(t)$ is the concentration of the product B.

The nonlinear model (1)–(2) of the isothermal Van de Vusse CSTR is a frequently used benchmark problem in nonlinear control (Kravaris and Daoutidis, 1990; Doyle *et al.*, 1995; Kravaris *et al.*, 1998; Perez *et al.*, 2002) due to challenging properties like multiple stationary setpoints and nonminimum–phase behavior.

2.1 Input–output normal form

The inversion–based feedforward control design is based on the input-output representation of the considered system. The CSTR model (1)–(2) is already in input–output normal form (Isidori, 1995) with relative degree $r = 1$ for $c_B > 0$. By use of the conventional coordinates $y = c_B$, $\eta = c_A$, the nonlinear input–output normal form

$$\dot{y} = k_1 \eta - k_2 y - y u, \qquad (3)$$

$$\dot{\eta} = -k_1 \eta - k_3 \eta^2 + (1 - \eta)u \qquad (4)$$

of the CSTR comprises the input–output dynamics and the internal dynamics. The inverse of the input–output dynamics (3) enables the algebraic calculation of the nominal input

$$u^* = \left(k_1 \eta^* - k_2 y^* - \dot{y}^*\right) / y^* \qquad (5)$$

in dependence of a desired output trajectory $y^*(t) > 0$, its derivative $\dot{y}^*(t)$, and the trajectory $\eta^*(t)$ of the internal dynamics (4). Therefore, to find the input trajectory $u^*(t)$ that maintains exact output tracking of $y^*(t)$ requires the solution $\eta^*(t)$ of the associated internal dynamics

$$\dot{\eta}^* = -k_1 \eta^* - k_3 \eta^{*2} + \left(1 - \eta^*\right)\left(k_1 \eta^* - k_2 y^* - \dot{y}^*\right) / y^* \qquad (6)$$

with the output trajectory $y^*(t)$ and its derivative $\dot{y}^*(t)$ serving as inputs.

A characteristic feature of the Van de Vusse CSTR model concerns that the internal dynamics (6) may be stable or unstable depending on the respective trajectory $y^*(t)$ of the output. Therefore, it is difficult to solve (6) by numerical integration.

---

[2] Thereby, $k_3 = \bar{k}_3 c_{A0}$, and the model parameters $k_1 = 50\ \mathrm{h}^{-1}$, $k_2 = 100\ \mathrm{h}^{-1}$, $\bar{k}_3 = 10\ \frac{\mathrm{L}}{\mathrm{mol\,h}}$, $c_{A0} = 10\ \frac{\mathrm{mol}}{\mathrm{L}}$ are taken from (Perez *et al.*, 2002) .

2.2 Transition between stationary setpoints

The stationary setpoints (y_s, η_s, u_s) of the CSTR satisfy the equations

$$0 = \left(k_3 + \frac{k_1}{y_s}\right)\eta_s^2 - \left(k_2 - k_1 + \frac{k_1}{y_s}\right)\eta_s + k_2, \quad (7)$$

$$u_s = (k_1\eta_s - k_2 y_s)\,/\,y_s \quad (8)$$

which follow from (3)–(4), see also (Perez *et al.*, 2002). The solutions to (7) are the set of equilibrium points (y_s, η_s) depicted in Figure 1. It clearly shows the occurence of multiple stationary setpoints, i.e. two different states η_s of the internal dynamics may exist for one output value $y_s < 0.127$.

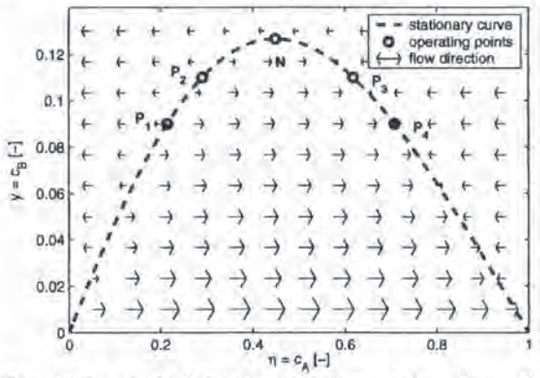

Fig. 1. Parabola (7) of equilibrium points (y_s, η_s) with flow direction and speed of the internal dynamics (6) for constant outputs y_s. The data of the stationary setpoints N and P_j, $j = 1, 2, 3, 4$ are given in Table 1.

Moreover, Figure 1 shows the flow of the internal dynamics (6) for constant outputs y_s. The internal dynamics is unstable for equilibrium points lying on the stationary curve to the left of point N, i.e. these equilibrium points have nonminimum–phase behavior. On the other hand, all equilibrium points to the right of N have stable internal dynamics and are minimum–phase, which can be directly seen by its flow direction.

Table 1. Data for stationary setpoints.

setpoints	$\eta_s = c_{As}$[–]	$y_s = c_{Bs}$ [-]	$u_s[\frac{1}{h}]$
P_1	0.215	0.090	19.6
P_2	0.292	0.110	32.6
N	0.450	0.127	78.0
P_3	0.618	0.110	180.9
P_4	0.708	0.090	293.6

Perez *et al.* (2002) investigated how to realize transitions between the stationary setpoints P_j, $j = 1, 2, 3, 4$ in Figure 1 by inversion–based feedforward control. Thereby, feasible and non–feasible transitions are distinguished in dependence of the stability properties of the internal dynamics at the respective setpoints. Feasible transitions concern e.g. $P_4 \to P_3$ and $P_2 \to P_1$, where both considered setpoints have the same stability property of the associated internal dynamics.

The transition between an initial and a terminal setpoint P_0 and P_T in Figure 1 within a finite–time interval $t \in [0, T]$ means that the output trajectory $y^*(t)$ and the internal dynamics (6) have to satisfy the boundary conditions (BCs)

$$y^*(0) = y_0, \quad y^*(T) = y_T, \quad \dot{y}^*|_{0,T} = 0, \quad (9)$$

$$\eta^*(0) = \eta_0, \quad \eta^*(T) = \eta_T. \quad (10)$$

The BCs $\dot{y}^*|_{0,T} = 0$ guarantee that the needed input trajectory $u^*(t)$ given in (5) is $\mathcal{C}^0$–continuous at the boundary points $t = 0, T$. [3]

From a mathematical point of view, the differential equation (6) together with the BCs (10) form a nonlinear two–point BVP for $\eta^*(t)$, $t \in [0, T]$ in dependence of the predefined output trajectory $y^*(t)$. As discussed in the following, the technique used for solving the BVP of the internal dynamics affects essentially the properties of the obtained feedforward control.

2.3 Feedforward design by stable system inversion

In (Perez *et al.*, 2002), the two–point BVP (6) and (10) is solved in an asymptotical manner following the idea of the stable inversion technique (Devasia *et al.*, 1996; Chen and Paden, 1996). Thereby, a suitable output trajectory $y^*(t)$ is predefined which satisfies the four BCs (9), e.g. by means of the third order polynomial [4]

$$y^*(t) = y_0 + (y_T - y_0)\sum_{i=2}^{3} a_i \left(\frac{t}{T}\right)^k \quad (11)$$

for $t \in [0, T]$, and with parameters $a_2 = 3$ and $a_3 = -2$ in order to satisfy the conditions $y^*(T) = y_T$ and $\dot{y}^*(T) = 0$.

The internal dynamics (6) is treated as an initial or terminal value problem where one of the BCs (10) is realized only asymptotically. If the internal dynamics is stable in both equilibrium points, Equation (6) can be numerically integrated forward in time $t \in [0, \infty)$ with the initial condition $\eta^*(0) = \eta_0$. The solution can be formally represented as

$$\eta^*(t) = \eta_0 + \int_0^t \beta(\eta^*(\tau), y^*(\tau), \dot{y}^*(\tau))\,\mathrm{d}\tau, \quad (12)$$

where the function $\beta(\cdot)$ abbreviates the right–hand side of (6). The solution $\eta^*(t)$ reaches the

[3] If discontinuities of $u^*(t)$ at $t = 0, T$ are allowed, the BCs $\dot{y}^*|_{0,T} = 0$ are omitted.

[4] In (Perez *et al.*, 2002), a ramp function is used to construct the output trajectory $y^*(t)$ which causes discontinuities of the input trajectory $u^*(t)$ at $t = 0, T$.

terminal value η_T only asymptotically for $t \to \infty$, as shown in Figure 2 for the transition $P_4 \to P_3$.

If the setpoints P_0 and P_T lie to the left of N, e.g. $P_2 \to P_1$, the internal dynamics is unstable in both stationary setpoints. Then, the internal dynamics (6) is integrated in reverse–time $t \in [T, -\infty)$ beginning with the terminal condition $\eta^*(T) = \eta_T$, i.e.

$$\eta^*(t) = \eta_T + \int_T^t \beta(\eta^*(\tau), y^*(\tau), \dot{y}^*(\tau))\mathrm{d}\tau. \quad (13)$$

This solution reaches the initial value η_0 only asymptotically for $t \to -\infty$, as depicted in Figure 2 for the transition $P_2 \to P_1$.

The asymptotic solution of the internal dynamics results either in an infinite postactuation or preactuation extension of the transition interval $t \in [0, T]$. Consequently, the input trajectories $u^*(t)$ are not constant outside the finite–time transition interval, although the output transition is performed as predefined. Due to this property, the designed feedforward trajectories $u^*(t)$ can only be implemented in an approximate manner.

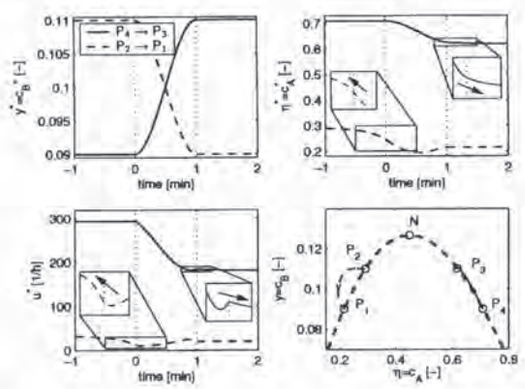

Fig. 2. Transition trajectories of output $y^*(t)$, internal dynamics $\eta^*(t)$, and input $u^*(t)$ calculated by numerical integrations (12) and (13).

The asymptotic solution technique fails if multiple equilibrium points are involved. This can be explained for the transitions $P_4 \to P_2$ and $P_4 \to P_3$ where the terminal points P_2 and P_3 possess the same y–coordinate. Therefore, the predefined trajectory $y^*(t)$ in (11) is identical for both transitions. Since the internal dynamics at the initial setpoint P_4 is stable, the numerical solution (12) in forward time can be used. However, the solution $\eta^*(t)$ will rather converge to the η–coordinate of P_3 instead of to the η–coordinate of P_2. In (Perez *et al.*, 2002), the transition $P_4 \to P_2$ is classified as non–feasible, but it will be used as benchmark scenario for the two alternative approaches of feedforward design presented in the following.

3. FLATNESS–BASED DESIGN OF FEEDFORWARD CONTROL

The Van de Vusse reactor model (3)–(4) is differentially flat and a flat output is given by (Rothfuss *et al.*, 1996)

$$z = (1 - \eta) / y \quad (14)$$

with respect to the coordinates $y = c_B > 0$ and $\eta = c_A$. Note that the fictitious output z bears a physical meaning and can be interpreted as the normalized inverse selectivity of the reaction between the substances A and B. The flat output (14) enables the purely algebraic parametrization of the trajectories

$$y^* = \psi_1(z^*, \dot{z}^*), \quad u^* = \psi_2(z^*, \dot{z}^*, \ddot{z}^*) \quad (15)$$

of the output and the input in dependence of the trajectory $z^*(t)$ and its derivatives $\dot{z}^*(t)$ and $\ddot{z}^*(t)$. [5]

The flatness–based design of feedforward control comprises the planning of a flat output trajectory $z^*(t)$ and the calculation of the output and input trajectories by means of the parametrizations (15) (Fliess and Marquez, 2000; Hagenmeyer and Zeitz, 2004).

At first, the BCs (9)–(10) of the considered transition have to be expressed in the flat output coordinate (14):

$$z^*(0) = z_0 = (1 - \eta_0)/y_0, \quad (16)$$

$$z^*(T) = z_T = (1 - \eta_T)/y_T, \quad (17)$$

$$\dot{z}^*|_{0,T} = 0, \quad \ddot{z}^*|_{0,T} = 0. \quad (18)$$

Then, a $\mathcal{C}^2$–trajectory $z^*(t)$ is set up as a fifth order polynomial

$$z^*(t) = z_0 + (z_T - z_0) \sum_{i=3}^{5} b_i \left(\frac{t}{T}\right)^i \quad (19)$$

for $t \in [0, T]$, whereby the coefficients $b_3 = 10$, $b_4 = -15$, and $b_5 = 6$ are chosen such that the terminal conditions in (17)–(18) are met. Finally, the trajectories $u^*(t)$ and $y^*(t)$ are obtained by purely algebraic evaluation of (15) using (19). The flatness–based feedforward control enables a finite–time transition between all setpoints of the Van de Vusse CSTR in Figure 1 without any time integration.

Figure 3 exemplarily shows the challenging transition $P_4 \to P_2$ for different transition times T. In the y–η–plane, the solution $(y^*(t), \eta^*(t))$ bypasses the stationary parabola (7) and approaches it for

[5] The functions $\psi_{1,2}(\cdot)$ can be determined by means of a computer algebra tool. The resulting expressions are quite vaste and are therefore abbreviated characterizing only their functional dependency.

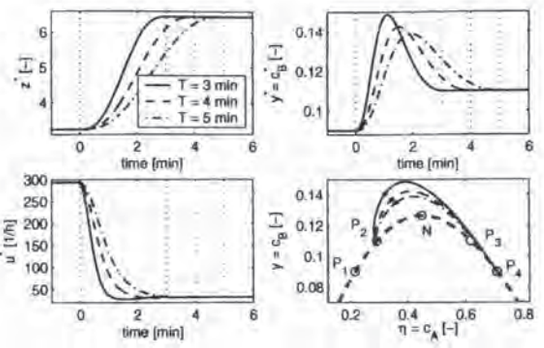

Fig. 3. Transition trajectories of flat output $z^*(t)$, input $u^*(t)$, and real output $y^*(t)$ for the transition $P_4 \rightarrow P_2$ by flatness–based feedforward control.

larger transition times T. Moreover, the input trajectory $u^*(t)$ is causal and constant for $t \notin [0, T]$, i.e. outside the transition interval, such that $u^*(t)$ can be exactly implemented.

Note that the output trajectory $y^*(t)$ follows from the constructed trajectory $z^*(t)$ of the flat output. Therefore, the shape of $y^*(t)$ must be checked in dependence of the parameters used in the set–up of $z^*(t)$. In Figure 3, the relation between the transition time T and the overshoot of $y^*(t)$ becomes evident.

4. A NEW APPROACH TO FEEDFORWARD CONTROL DESIGN

The main idea of the second design approach which is not restricted to flat systems concerns to exactly solve the two–point BVP (6) and (10) of the internal dynamics. Thereby, a free parameter p is provided in the set–up of the predefined output trajectory $y^*(t, p)$ such that the BVP of the internal dynamics is solvable (Graichen *et al.*, 2004). In order to elaborate the difference to the predefined polynomial set–up (11), the new set–up is split into two parts

$$y^*(t, p) = \hat{y}^*(t) + \tilde{y}(t, p), \quad t \in [0, T]. \tag{20}$$

The first part $\hat{y}^*(t)$ represents a predefined output trajectory which is constructed according to (11). The variation $\tilde{y}(t, p)$ contains the free parameter p and must satisfy the homogeneous BCs

$$\tilde{y}(0, p) = 0, \quad \tilde{y}(T, p) = 0, \quad \dot{\tilde{y}}|_{0,T} = 0. \tag{21}$$

The four BCs would require a third order polynomial for the construction of $\tilde{y}(t, p)$. In order to provide the free parameter p, the polynomial is extended up to forth order

$$\tilde{y}(t, p) = \sum_{i=2}^{3} \tilde{a}_i(p) \left(\frac{t}{T}\right)^i + p \left(\frac{t}{T}\right)^4 \tag{22}$$

for $t \in [0, T]$. The coefficients $\tilde{a}_2(p) = p$ and $\tilde{a}_3(p) = -2p$ depend on the parameter p such that $\tilde{y}(t, p)$ satisfies the two terminal conditions in (21) at $t = T$.

The splitting (20) of the output trajectory $y^*(t, p)$ enables a separate set–up of the functions $\hat{y}^*(t)$ and $\tilde{y}(t, p)$. For instance, smooth Gevrey functions (Gevrey, 1918) may be used for a predefined trajectory $\hat{y}^*(t) \in \mathcal{C}^\infty$, whereas the variation function $\tilde{y}(t, p)$ can be designed by use of polynomial, spline, or trigonometric functions.

The modified BVP of the internal dynamics is obtained if the trajectory $y^*(t)$ is substituted in (6) by the trajectory $y^*(t, p)$, and the associated BCs (10) are considered. A difficult issue is the solvability of nonlinear two–point BVPs. In case of the Van de Vusse example, the BVP is well–posed and the existence of a solution is guaranteed since the reactor model (1)–(2) is differentially flat (see previous section) which corresponds to its controllability for $y > 0$.

The standard MATLAB function bvp4c [6] is used to solve the two–point BVP (6), (10), (20)–(22) with an unknown parameter p. The BVP solver bvp4c employs a collocation formula and solves a set of nonlinear algebraic equations. The solution is $\mathcal{C}^1$–continuous and forth order accurate uniformly in the interval of the considered BVP. Mesh selection and error control are based on the residual of the continuous solution. If the solution does not satisfy the tolerance criteria, the solver adapts the mesh. The user must provide the initial points of the mesh as well as a guess of the solution at the mesh points and of the unknown parameter.

Finally, the solutions $\eta^*(t)$ and p^* are used to calculate the input trajectory

$$u^*(t) = \frac{k_1 \eta^*(t) - k_2 y^*(t, p^*) - \dot{y}^*(t, p^*)}{y^*(t, p^*)} \tag{23}$$

by inserting $\eta^*(t)$ and $y^*(t, p^*)$ in (5). Thereby, the condition $y^*(t, p^*) > 0$ has to be checked and fulfilled. In contrast to the asymptotic solutions (12) and (13), the new approach determines the trajectory $\eta^*(t)$ on $t \in [0, T]$ such that the BCs (10) at both bounds $t = 0$ and $t = T$ are met. Therefore, the feedforward control trajectory $u^*(t)$ in (23) is causal, constant for $t \notin [0, T]$, and therefore also implementable.

The trajectories for the challenging transition problem $P_4 \rightarrow P_2$ are depicted in Figure 4 for three different transition times T. The variation function $\tilde{y}(t, p^*)$ significantly distorts the predefined output trajectory $\hat{y}^*(t)$, since the flow $(y^*(t, p^*), \eta^*(t))$ bypasses the maximum point N in the η–y–plane which requires a considerable overshoot in the output trajectory $y^*(t, p^*)$. This scenario clearly shows that the variation func-

[6] ftp://ftp.mathworks.com/pub/doc/papers/bvp/

tion $\tilde{y}(t, p^*)$ accounts for the internal dynamics in course of the transition.

It is stressed that the new design approach does not distinguish between stable or unstable internal dynamics, since its trajectory $\eta^*(t)$ is determined purely algebraically without an integration over the time–coordinate. Therefore, the new approach works equally well for all setpoint transitions $P_0 \rightarrow P_T$ of the Van de Vusse CSTR in Figure 1.

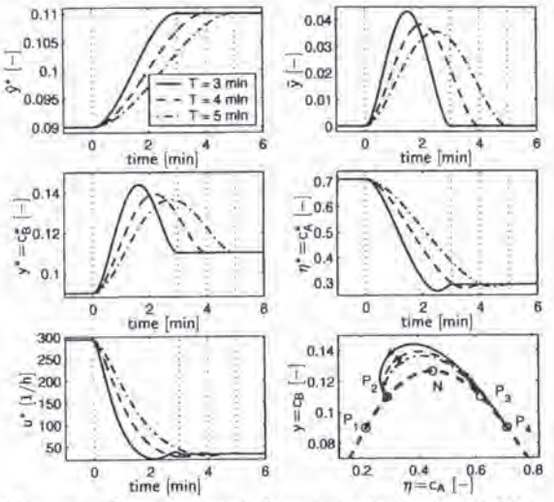

Fig. 4. Output and input trajectories $\hat{y}^*(t)$, $\tilde{y}(t, p^*)$, $y^*(t, p^*)$, and $u^*(t)$ for the transition $P_2 \rightarrow P_4$ by the new design approach for feedforward control.

5. CONCLUSIONS

Both presented design approaches of nonlinear feedforward control are purely algebraic and can be employed for minimum–phase and nonminimum–phase systems. The two approaches deliver feedforward input trajectories without pre–transition and post–transition intervals such that they can be exactly implemented. Finally, it is possible to provide additional parameters in the set–up of the predefined trajectories of both approaches in order to optimize a cost function as it is investigated in (Perez *et al.*, 2002). At any rate, the flatness–based design requires that the considered system is differentially flat, whereas the second approach can be applied to a more general class of nonlinear sytems.

ACKNOWLEDGEMENTS

The authors gratefully thank Thomas Meurer and Marc Oliver Wagner for useful hints and discussions.

REFERENCES

Chen, D. and B. Paden (1996). Stable inversion of nonlinear non–minimum phase systems. *Int. J. Contr.* **64**, 81–97.

Devasia, S. (1999). Approximated stable inversion for nonlinear systems with nonhyperbolic internal dynamics. *IEEE Trans. Automat. Contr.* **44**, 1419–1425.

Devasia, S. and B. Paden (1998). Stable inversion for nonlinear nonminimum–phase time–varying systems. *IEEE Trans. Automat. Contr.* **43**, 283–288.

Devasia, S., D. Chen and B. Paden (1996). Nonlinear inversion–based output tracking. *IEEE Trans. Automat. Contr.* **41**, 930–942.

Doyle, F.J., B. Ogunnaike and R.K. Pearson (1995). Nonlinear model–based control using second–order volterra models. *Automatica* **31**, 697–714.

Fliess, M. and R. Marquez (2000). Continuous–time linear predictive control and flatness: a module-theoretic setting with examples. *Int. J. Contr.* **73**, 606–623.

Fliess, M., J. Lévine, P. Martin and P. Rouchon (1995). Flatness and defect of nonlinear systems: introductory theory and examples. *Int. J. Contr.* **61**, 1327–1361.

Gevrey, M. (1918). La nature analytique des solutions des équation aux dérivées partielles. *Annales Scientifiques de l'Ecole Normale Superieure* **25**, 129–190.

Graichen, K., V. Hagenmeyer and M. Zeitz (2004). A new approach to inversion–based feedforward control design for nonlinear systems (submitted).

Hagenmeyer, V. and M. Zeitz (2004). Flachheitsbasierter Entwurf von linearen und nichtlinearen Vorsteuerungen. *Automatisierungstechnik* **52**, 3–12.

Hunt, L.R. and G. Meyer (1997). Stable inversion for nonlinear systems. *Automatica* **33**, 1549–1554.

Isidori, A. (1995). *Nonlinear Control Systems.* 3rd ed.. Springer.

Kravaris, C. and P. Daoutidis (1990). Nonlinear state feedback control of second–order nonminimum–phase nonlinear systems. *Comput. Chem. Eng.* **14**, 439–449.

Kravaris, C., M. Niemiec, R. Berber and C.B. Brosilow (1998). Nonlinear model–based control of nonminimum–phase processes. In: *Nonlinear model based process control* (R. Berber and C. Kravaris, Eds.). Vol. 353. pp. 115–142. NATO ASI series.

Perez, H., B. Ogunnaike and S. Devasia (2002). Output tracking between operating points for nonlinear processes: Van de Vusse example. *IEEE Trans. Contr. Syst. Techn.* **10**, 611–617.

Rothfuss, R., J. Rudolph and M. Zeitz (1996). Flatness based control of a nonlinear chemical reactor model. *Automatica* **32**, 1433–1439.

Taylor, D.G. and S. Li (2002). Stable inversion of continuous–time nonlinear systems by finite–difference methods. *IEEE Trans. Automat. Contr.* **47**, 537–542.

Zou, Q. and S. Devasia (1999). Preview–based stable–inversion for output tracking. *ASME J. Dyn. Syst. Meas. Contr.* **121**, 625–630.